

Robust chirped mirrors

Omid Nohadani,^{1,*} Jonathan R. Birge,² Franz X. Kärtner,² and Dimitris J. Bertsimas¹

¹Operations Research Center and Sloan School of Management, Massachusetts Institute of Technology,
77 Massachusetts Avenue, Cambridge, Massachusetts, USA

²Research Laboratory of Electronics and Department of Electrical and Computer Engineering, Massachusetts Institute of
Technology, 77 Massachusetts Avenue, Cambridge, Massachusetts, USA

*Corresponding author: nohadani@mit.edu

Received 19 December 2007; revised 4 March 2008; accepted 7 March 2008;
posted 10 March 2008 (Doc. ID 91029); published 6 May 2008

Optimized chirped mirrors may perform suboptimally, or completely fail to satisfy specifications, when manufacturing errors are encountered. We present a robust optimization method for designing these dispersion-compensating mirror systems that are used in ultrashort pulse lasers. Possible implementation errors in layer thickness are taken into account within an uncertainty set. The algorithm identifies worst-case scenarios with respect to reflectivity as well as group delay. An iterative update improves the robustness and warrants a high manufacturing yield, even when the encountered errors are larger than anticipated. © 2008 Optical Society of America
OCIS codes: 310.4165, 310.6860, 320.0320.

1. Introduction

The dispersion-compensating mirror, first proposed in 1994 [1], has become an enabling technology for modern ultrafast lasers. Solid-state mode-locked lasers can only operate at or below few-cycle pulse widths when the total cavity dispersion is reduced to nearly zero, with only a small amount (on the order of a few fs²) of residual second-order dispersion. While prisms can be used to compensate for second- and third-order cavity dispersion, their relatively high loss and inability to compensate for arbitrary dispersion limits their use; pulse durations below 10 fsec were not possible directly from oscillators until the development of high performance double-chirped mirror pairs [2–4].

As bandwidths increase, so do the number of layers required to produce a mirror with the high reflectivity needed for an intracavity mirror. For bandwidths exceeding an octave, mirror pairs with over 200 total layers are generally required. The sensi-

tivity of a dielectric stack to manufacturing errors increases with the number of layers, and dispersion-compensating mirrors push the limits of manufacturing tolerances, requiring layer precisions on the order of a nanometer. Currently, this challenges even the best manufacturers.

While the nominal optimization of layer thickness has led to successful design of dispersion-compensating dielectric mirrors allowing dispersion and reflectivity control over nearly an octave of bandwidth, in practice the performance for such complicated mirrors is limited by the manufacturing tolerances of the mirrors. Small perturbations in layer thickness not only result in suboptimal designs, but due to the nonlinear nature of mode-locking, such perturbation may completely destroy the phenomenon.

Despite the fact that manufacturing errors often limit the performance of thin-film devices [5], there has been little work on optimizing thin-film designs to mitigate the effects of errors. Some previous work in designing fault-tolerant mirrors has focused on optimizing first-order tolerances, a method readily available in commercial thin-film design codes [6].

Our approach to robust optimization probes the exact merit function in a bounded space of potential

0003-6935/08/142630-07\$15.00/0
© 2008 Optical Society of America

thickness errors. While this results in a much more computationally involved optimization, the result is arguably more robust to significant perturbation as the full structure of the merit function is considered in a neighborhood around a nominal solution. Furthermore, the robustness is guaranteed to be equal or better than that obtained with nominal optimization, and in the case where it is equal, no sacrifice in nominal optimality will be made.

Other prior work was done by Yakovlev and Tempea [7], who employed stochastic global optimization to achieve robustness of the final solution by virtue of the fact that they optimized a Monte Carlo computed integral over a neighborhood around a nominal design. Their method does not suffer the limitations of first-order tolerances, and was able to produce mirrors with significant improvement over nominally optimized designs, demonstrating conclusively that robustness can be greatly improved at the design level by proper optimization.

Ben-Tal and Nemirovski provided a first robust optimization approach based on an application in antenna design [8]. Recent works have been devoted to problems with convex objectives and constraints (e.g., linear) [9–11]. These works have shown that a convex optimization problem with parameter uncertainty can be transformed to another convex optimization problem. Despite significant advancements, all these results are limited to convex problems. But modern engineering design often involves problems with objectives and constraints that are not explicitly given and highly nonconvex. Thus, no internal structure can be exploited.

We present a new deterministic robust optimization method that provides for designs which are intrinsically protected against potentially significant layer-thickness perturbations occurring during manufacturing. The presented method is generic and can be applied to many problems that are solved through numerical simulations [12]. Here, we introduce the algorithm specifically for double-chirped mirrors and tailor the parameters to this particular problem. First, we discuss the optical properties of these mirrors and define a cost function based on reflectivity and group delay. We continue with the introduction of the concept of the uncertainty set as well as a novel method to identify worst-case designs within this set. Once these configurations are found, we show how an update direction can be found which eliminates these worst cases. Furthermore, we demonstrate the performance of the nominal and robust solutions for a large range of perturbation and propose a technique to increase the manufacturing yield.

2. Computation of Cost Function

The cost function for a chirped mirror is typically composed of two terms, one representing the performance of the reflectivity (which is ideally one) and another which quantifies the deviation of the

dispersion from ideal. We employ a cost or merit function than is given as

$$f(\mathbf{x}) = \sum_k w_r(\lambda_k) [R(\lambda_k; \mathbf{x}) - 1]^4 + \sum_k w_d(\lambda_k) [\tau_g(\lambda_k; \mathbf{x}) - \hat{\tau}_g(\lambda_k) + \tau_0(\mathbf{x})]^2, \quad (1)$$

where $R(\lambda; \mathbf{x})$ is the wavelength domain reflectivity of the total mirror pair described by layer thicknesses \mathbf{x} , $\tau_g(\lambda; \mathbf{x})$ is the group delay (GD) of the pair, $\hat{\tau}_g(\lambda)$ is the ideal GD, and the $w_{r,d}(\lambda)$ are weighting functions. To account for an irrelevant offset between the computed and ideal group delay curves, we include a constant offset, $\tau_0(\mathbf{x})$, that minimizes the error. For the reflectivity errors, we use the fourth power of the error to approximate a Chebychev norm, though a standard squared error can also be used.

The computation of reflectivity from a thin-film stack is done using transfer matrix methods [13]. In a standard nominal optimization, the merit function and its gradient must be evaluated thousands of times over hundreds of wavelengths. In a robust optimization, the computational burden is even greater, with the merit function typically computed on the order of a million times. Any discrepancy in the gradient will hinder the convergence rate. Thus, it is imperative that the merit function be computed efficiently and accurately. We employ the methods described in [14,15], where the group delay is computed in an approximate analytic form that allows for a significant reduction in computational complexity. The approximation simply neglects the local change in wavelength of the Fresnel reflections between each layer. For chirped mirrors, the approximation error is negligible, as demonstrated and explained in [14]. The gradient of the group delay is computed analytically in a self-consistent manner with the approximation, resulting in an optimization that converges quickly, both in terms of iterations and total processing time.

3. Problem Statement

Our design problem consists of a double-chirped mirror pair with 208 layers for use in a few-cycle titanium:sapphire mode-locked laser [16]. The initial design was computed using the analytic method of [4]. The materials used were SiO_2 and TaO_5 , with the dispersion of each modeled using Sellmeier coefficients obtained from fits to manufacturer's index data. The total reflection dispersion of the pair is specified to compensate for 2.2 mm of Titanium:sapphire, 2 m of air, and 8 mm of Barium Fluoride in a cavity containing six mirrors. The group delay and reflectivity are optimized over 156 wavelengths, uniformly spaced from 650 to 1200 nm. This discretization was empirically found to be sufficient to avoid narrow resonances "leaking" through the grid. The angle of incidence is taken to be 6° , and

the polarization is assumed to be transverse in the magnetic field (TM). The reflectivity and group delay are optimized as in Eq. (1), with constant weightings $w_r = 1$ and $w_d = 10^{-8} \text{ fs}^{-2}$.

4. Implementation Errors

A. General Model

For the purposes of developing this algorithm, we model manufacturing errors as independent random sources of additive noise, since any known systematic errors, such as miscalibration, can be best addressed in the actual production. As empirically supported, the layer-thickness errors can be regarded as not correlated. Therefore, we assume that when manufacturing a mirror with layer thicknesses given by \mathbf{x} , statistically independent additive implementation errors $\Delta\mathbf{x} \in \mathbb{R}^n$ may be introduced due to variation in the coating process, resulting in an actual thicknesses $\mathbf{x} + \Delta\mathbf{x}$. We assume a mean of zero and a variance on each layer that is motivated by actual manufacturing errors. Here, $\Delta\mathbf{x}$ resides within an uncertainty set

$$\mathcal{U} := \{\Delta\mathbf{x} \in \mathbb{R}^n \mid \|\Delta\mathbf{x}\|_2 \leq \Gamma\}, \quad (2)$$

where $\|\cdot\|_2$ is the Euclidean norm. Note that $\Gamma > 0$ is a scalar describing the size of perturbation against which the design needs to be protected. For this paper, we took the manufacturing uncertainty to be normally distributed with a standard deviation of $\sigma = 0.5 \text{ nm}$. To maintain 95% cumulative confidence to capture all errors within \mathcal{U} for this 208-dimensional problem, we chose $\Gamma = 0.0075 \mu\text{m}$. We seek a robust design of x by minimizing the worst-case cost

$$g(\mathbf{x}) := \max_{\Delta\mathbf{x} \in \mathcal{U}} f(\mathbf{x} + \Delta\mathbf{x}). \quad (3)$$

The worst-case cost $g(x)$ is the maximum possible cost of implementing \mathbf{x} due to an error $\Delta\mathbf{x} \in \mathcal{U}$. Thus, the robust optimization problem is given through

$$\min_{\mathbf{x}} g(\mathbf{x}) \equiv \min_{\mathbf{x}} \max_{\Delta\mathbf{x} \in \mathcal{U}} f(\mathbf{x} + \Delta\mathbf{x}). \quad (4)$$

In other words, the robust optimization method seeks to minimize the worst-case cost. When implementing a certain design $\mathbf{x} = \hat{\mathbf{x}}$, the possible realization due to implementation errors $\Delta\mathbf{x} \in \mathcal{U}$ lies in the set

$$\mathcal{N} := \{\mathbf{x} \mid \|\mathbf{x} - \hat{\mathbf{x}}\|_2 \leq \Gamma\}. \quad (5)$$

We call \mathcal{N} the neighborhood of $\hat{\mathbf{x}}$; such a neighborhood is illustrated in Fig. 1. A design \mathbf{x} is a neighbor of $\hat{\mathbf{x}}$ if it is in \mathcal{N} . Therefore, $g(\hat{\mathbf{x}})$, is the maximum cost attained within \mathcal{N} . Let $\Delta\mathbf{x}^*$ be one of the worst implementation errors at $\hat{\mathbf{x}}$, $\Delta\mathbf{x}^* = \arg \max_{\Delta\mathbf{x} \in \mathcal{U}} f(\hat{\mathbf{x}} + \Delta\mathbf{x})$. Then, $g(\hat{\mathbf{x}})$ is given by $f(\hat{\mathbf{x}} + \Delta\mathbf{x}^*)$.

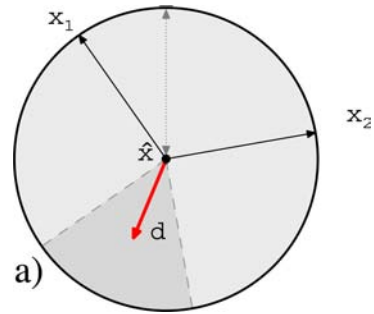


Fig. 1. (Color online) Two-dimensional illustration of the neighborhood. For a design $\hat{\mathbf{x}}$, all possible implementation errors $\Delta\mathbf{x} \in \mathcal{U}$ are contained in the shaded circle. The bold arrow d shows a possible descent direction and thin arrows $\Delta\mathbf{x}_i^*$ represent worst errors.

Since we seek to navigate away from all the worst implementation errors, the inner maximization problem needs to be solved first. Given that f is nonconvex and provided through numerical calculations, we cannot exploit any possible internal structure to compute g . Therefore, we conduct local searches to determine worst configurations within \mathcal{N} .

Previously, it was shown that all worst-case scenarios reside on the shell of \mathcal{N} [17]. Thus, to improve the speed of the inner maximization, we can restrict ourselves to only considering error vectors $\Delta\mathbf{x}$ such that the $\|\Delta\mathbf{x}\|_2 = \Gamma$. Problem (4) then transforms into a constrained maximization over the shell $\|\Delta\mathbf{x}\|_2 = \Gamma$, which makes the search more computationally efficient.

B. Restricted Search Space

To protect a design against errors, it is helpful to utilize available understanding of possible errors. For example, if there are worst-case scenarios in the respective neighborhood that are very rare according to our assumed layer perturbation distribution, there is no need for them to be considered during the inner maximization problem (3). By excluding these rare events from \mathcal{U} , we are able to protect the design against realistic and statistically relevant errors only, without needlessly sacrificing nominal performance to guard against rare errors. Moreover, this approach leads to a reduction of the size of the respective search space and, thus, to an increase of the computational efficiency.

It is well known that the reflection coefficients of thin-film stacks are closely related to the Fourier transform of the layer thicknesses [18]. Thus, one promising class of rare perturbations to eliminate from consideration are those which have strong correlations between the layers. These errors involve, for example, shifting of all the thicknesses in one direction, which results in a spectral shift regardless of the design. Even though such errors may occur in actual manufacturing due to systematic issues, there is little or nothing that can be done to deal with them by design optimization, and to attempt to do so will only result in a highly compromised design. We thus restrict ourselves to considering only statistically independent random perturbations to the layers.

In this context, the probability of errors occurring with high correlation between the layers is negligible, and thus we should not concern ourselves with protecting against them. We therefore seek a class of errors which restricts the allowable correlation between layers, i.e., we restrict the maximum variation in the amplitude of the Fourier components of the error vector. A straightforward way to do this is to restrict the search to the class of error vectors with minimum coherence, requiring all Fourier components to have a uniform amplitude.

In addition to the above, this choice of subset is justified empirically. Monte Carlo simulations reveal that the set of perturbations with uniform amplitude in the Fourier domain with uniformly distributed phases have virtually identical statistics to the general uncertainty set \mathcal{U} defined in Eq. (2). The cumulative probability distribution of the reduced set never exceeds the full set by more than 4%. This confirms that our worst-case search over the reduced subset will not miss anything statistically relevant in the full set, and thus robustness is not compromised by using this set.

In the restricted space, the components of Δx can be written as

$$\Delta x_j = \frac{\Gamma}{[N/2]} \sum_{k=1}^{[N/2]} \cos\left(\frac{2\pi k j}{N} + \phi_k\right), \quad (6)$$

where ϕ_k is the phase of the k th Fourier component of Δx and N is the number of layers. We furthermore assume the constant (zero frequency) component is zero, which corresponds to the aforementioned pathological case of all layers shifting a similar amount. Using Parseval's theorem, i.e., the sum of the square of a function is equal to the sum of the square of its transform, we can verify that the magnitude of the errors remains on the shell of the original uncertainty set \mathcal{U} ,

$$\|\Delta \mathbf{x}\|_2^2 = \sum_{k=1}^N |\Delta x_k|^2 = \Gamma^2. \quad (7)$$

Using this transformation, we search over the phases ϕ_k for worst-case neighbors. Therefore, the search space dimensionality is reduced to $[N/2]$; hence, the efficiency of this algorithm increases by N^2 . Most importantly, since the maximization problem is over the free phase-space on the shell and the magnitude of these vectors are constant, the advantages of an unconstrained search can be exploited. Consequently, we obtain the set of local maxima in the phase space using standard gradient-based optimization. Furthermore, we obtain a set of true bad neighbors, which is significantly smaller in size ($\ll 500$) than had we left the search space more general. Since this size determines the number of constraints in the problem, we experience a significant speed up in this part of the algorithm as well.

5. Robust Optimization

Once worst-case neighbors are identified, a direction is sought along which an updated neighborhood would not include these worst-case scenarios any longer. This direction is a vector that spans the largest angle $\Theta \geq 90^\circ$ to all worst implementation errors at $\hat{\mathbf{x}}$ in the set of worst implementation errors

$$\mathcal{U}^*(\hat{\mathbf{x}}) := \{\Delta \mathbf{x}^* | \Delta \mathbf{x}^* = \arg \max_{\Delta \mathbf{x} \in \mathcal{U}} f(\hat{\mathbf{x}} + \Delta \mathbf{x})\}. \quad (8)$$

To navigate away from the elements in $\mathcal{U}^*(\hat{\mathbf{x}})$, a descent direction \mathbf{d}^* can be found efficiently by solving the following second-order cone problem (SOCP):

$$\begin{aligned} & \underset{\mathbf{d}, \beta}{\text{minimize}} && \beta \\ & \text{subject to} && \|\mathbf{d}\|_2 \leq 1 \\ & && \mathbf{d} \Delta \mathbf{x}^* \leq \beta \quad \forall \Delta \mathbf{x}^* \in \mathcal{U}^*(\hat{\mathbf{x}}) \\ & && \beta \leq -\epsilon, \end{aligned} \quad (9)$$

where ϵ is a small positive scalar and β is an auxiliary variable. A feasible solution to problem (9), \mathbf{d}^* , forms the maximum possible angle θ_{\max} with all $\Delta \mathbf{x}^*$, as illustrated in Fig. 1. This angle is always greater than 90° due to the constraint $\beta \leq -\epsilon < 0$. This constraint guarantees that \mathbf{d}^* will provide an updated design neighborhood that excludes all known $\Delta \mathbf{x}^*$. The value of ϵ is chosen heuristically such that when problem (9) is infeasible, then $\hat{\mathbf{x}}$ is a robust local minimum. Note, that the constraint $\|\mathbf{d}^*\|_2 = 1$ is automatically satisfied if the problem is feasible. Such an SOCP can be solved efficiently using both commercial and noncommercial solvers, e.g., [19]. Because $\Delta \mathbf{x}^*$ usually reside among designs with nominal costs higher than the rest of the neighborhood, the following algorithm summarizes a heuristic strategy for the robust local search [17]:

Algorithm 1

Step 0—Initialization: Let \mathbf{x}^1 be an arbitrarily chosen initial decision vector. Set $k:=1$.

Step 1—Neighborhood Exploration: Find a set of implementation errors $\Delta \mathbf{x}_i$ with the highest cost within the neighborhood of \mathbf{x}^k . For this, we conduct multiple unconstrained maximization searches over the shell of the uncertainty set starting from random initial configurations. The results of all function evaluations $(\mathbf{x}, f(\mathbf{x}))$ are recorded in a bad-neighbors set.

Step 2—Robust Local Move:

- i. Solve the SOCP (9); terminate if the problem is infeasible
- ii. Set $\mathbf{x}^{k+1} := \mathbf{x}^k + t^k \mathbf{d}^*$, where \mathbf{d}^* is the optimal solution to the SOCP.
- iii. Set $k:=k+1$. Go to Step 1.

The step size t^k is computed as the shortest step size that eliminates all bad neighbors from \mathbf{x}^k .

Reference [17] provides a detailed discussion on the actual implementation.

6. Results

Starting from a nominally optimized solution, our robust optimization algorithm successively decreased the worst-case cost, as in Eq. (3). This performance is shown in Fig. 2. The significant improvement of robustness comes at the price of a small increase in the nominal cost. The algorithm converges to the robust local minimum, at which point no descent direction can be found.

The reflectivity and group delay of the robust and nominal optimum are shown in Fig. 3. While both solutions satisfy the design objectives, the robust design is significantly more protected against possible errors. The unavoidable “price of robustness” through a decrease of the nominal performance of the robust solution is apparent, with increased ripple in the group delay and reflectivity. This price is especially apparent in the bottom plot of Fig. 3, which compares the total group delay error for the robust and nominally optimized mirror pairs. However, as

is shown in Figs. 5 and 6, the robust solution performs better when the layer perturbations are taken into account. Even though the nominally optimized design is able to achieve GD errors of less than 1 fsec, it turns out that the half nanometer layer perturbations we took as our assumed manufacturing tolerances result in GD errors on the order of plus or minus five femtoseconds.

In Fig. 4, we show the layer thicknesses for the mirror pair both after nominal optimization and robust optimization. The general structure of the mirror is preserved in the robust optimum solution, in keeping with the observation that its nominal performance is not degraded significantly. The larger variations are found in the first several layers, which perform impedance matching into the chirped stack, suggesting that they are the most sensitive to perturbation. This is consistent with the fact that any spurious reflections off of the front surface of the mirror will significantly degrade the GD performance.

While we intended to match the size of the uncertainty to the reported manufacturing and measurement errors, the value of Γ might not fully reflect

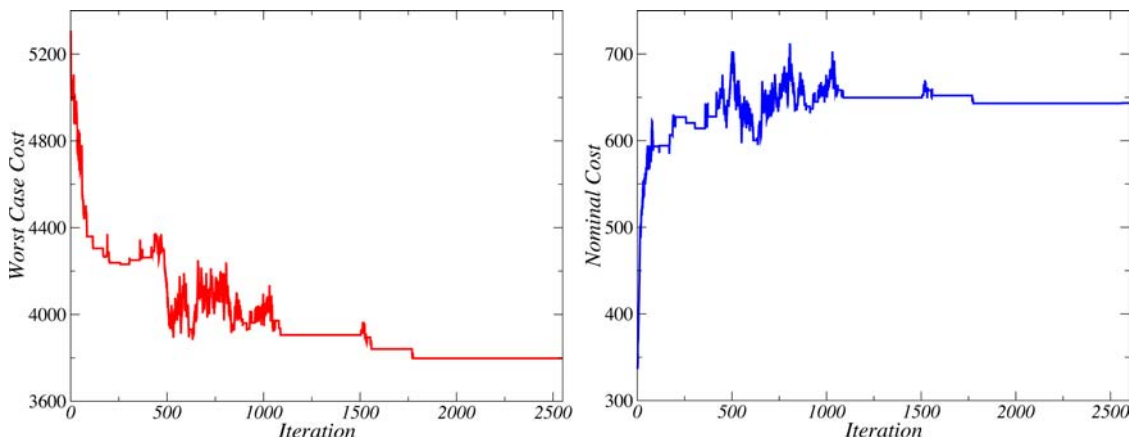


Fig. 2. (Color online) Robust optimization algorithm improves (left) the worst-case cost in the neighborhood of the current design. Discoveries of new bad neighbors cause the small peaks. (Right) The price of robustness is an increase in the nominal cost.

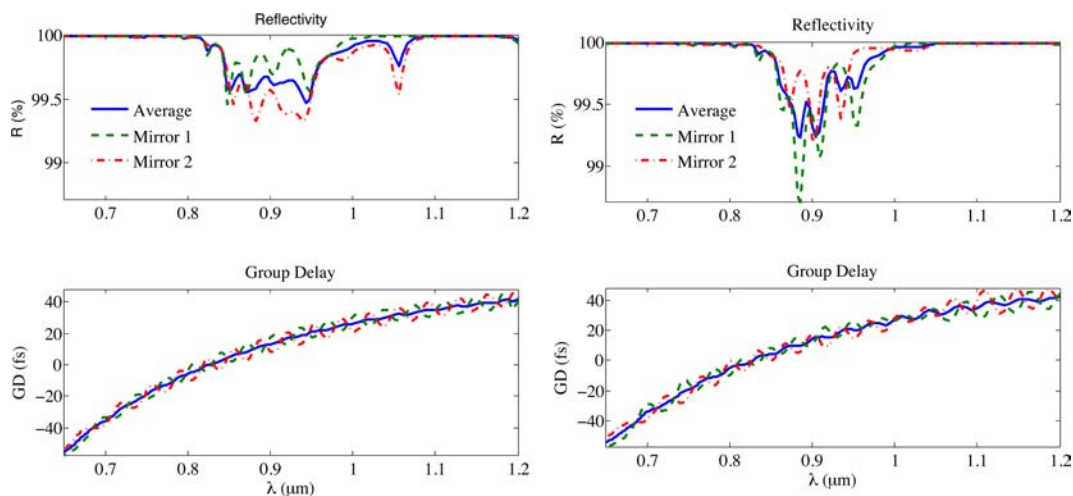


Fig. 3. (Color online) Reflectivity and group delay for each chirped mirror in the pair: (left) nominally optimal design; (right) robustly optimal configuration.

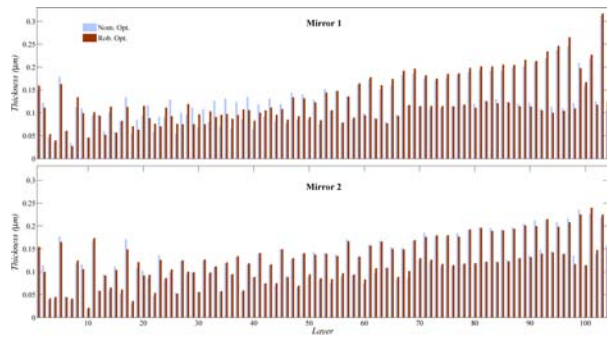


Fig. 4. (Color online) Layer thicknesses of nominal optimum and robust optimum of the mirror pair.

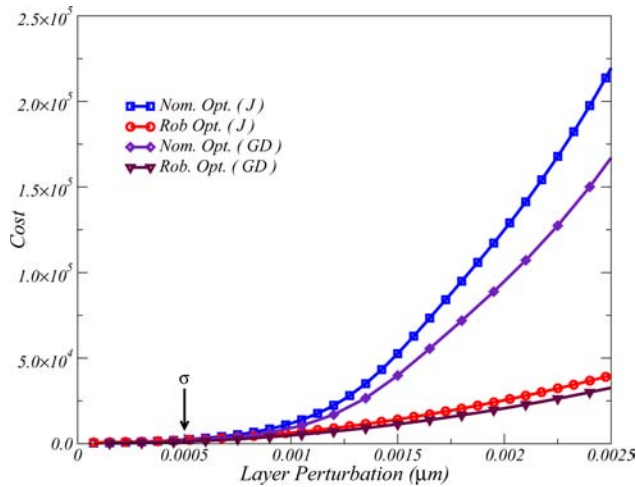


Fig. 5. (Color online) Comparison of worst-case cost and worst-case GD cost of two designs, the nominal and robust optimum, for increasing size of possible perturbations or errors.

the actual errors. Therefore, our algorithm seeks to find robust solutions with stable performance even beyond predicted errors. To illustrate these effects, we varied the size of the uncertainty set and evaluated the worst possible neighbor within this neighborhood. The worst-case scenarios of the nominal optimum and robust optimum, both in cost as well as the optical properties, are compared for increasing neighborhood size in Fig. 5.

The worst-case performance of both the nominal and robust designs behave fairly similarly within a small range of perturbations, which is in fact comparable to Γ . However, once the size of possible errors increases, the worst-case cost of the nominal design drastically rises, showing that this design would lose its phenomena completely.

Since any manufacturing process is to some extent statistical, it is essential for a design to yield a high manufacturing yield. Our robust optimization method not only minimizes the worst-case performance, but also addresses these statistical effects. This is demonstrated in Fig. 6. A series of Monte Carlo simulations, each with 10^6 randomly sampled designs with normally distributed layer perturbations, were performed with varying standard deviations at the robust and the nominal optimum. The

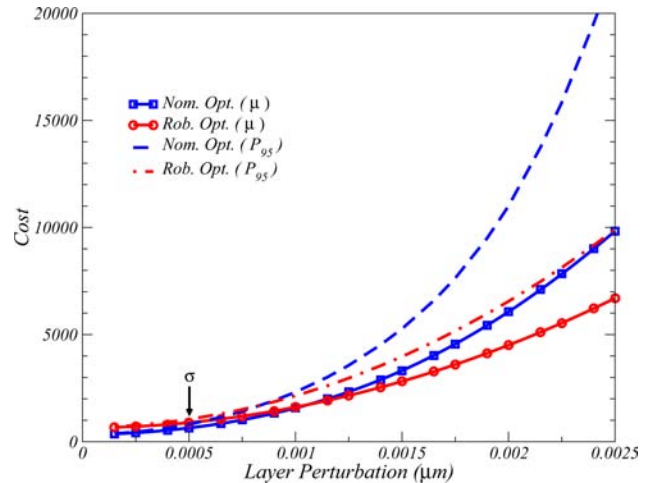


Fig. 6. (Color online) Comparison of the nominal and robust design: mean and ninety-fifth percentile of the cost distribution of 10^6 randomly sampled designs for varying perturbation sizes.

mean μ and the ninety-fifth percentile P_{95} of the distribution for each perturbation size are plotted to illustrate the center and the actual width of this statistical process. While both designs are similarly distributed within the expected errors σ , they deviate significantly beyond this mark. In fact, the mean and more importantly the spread of the distribution for the nominal optimum design increases rapidly beyond σ , while the robust optimum is more moderate. Moreover, the mean of the nominal optimum at all perturbation sizes is within the distribution (P_{95}) of the robust optimum, demonstrating that the manufacturing yield of the robust solution remains high and provides performances comparable to the nominal design, even beyond the assumed errors. Since the notion of the actual manufacturing errors are often somewhat uncertain, our method can provide a robust solution despite these uncertainties.

7. Conclusions

We have developed a new robust optimization technique specifically tailored to the problem of thin-film filter optimization. Our method obtains robust solutions by performing a series of deterministic gradient ascent searches around a given trial solution for worst-case errors. To avoid taking into account extremely rare potential errors, we perform this search over the space of all errors on the shell of our neighborhood whose components are minimally coherent. This avoids taking into account rare but highly significant errors, such as those associated with certain types of systematic manufacturing errors, which would otherwise dominate the optimization. This modification allows an unconstrained inner maximization over a reduced search space, and thus, improves the efficiency. Once, a set of worst-case designs are identified within an uncertainty set, our method provides an updated design that has reduced worst-case performance. After a number of iterations, we obtain a robust optimum that has the lowest worst-case performance.

We apply the method to a demanding optimization of a 208 layer chirped mirror pair with nearly an octave of bandwidth. The robust solution is compared with that obtained using standard optimization techniques, and is found to achieve improved statistical performance for layer errors of half a nanometer. Furthermore, the fault tolerance of the robust solution increases significantly relative to the nominally optimized mirror as the error variance increases, demonstrating that the robust solution is not tied to the particular manufacturing error variance assumed during optimization (see Fig. 6). Therefore, our robust design warrants for a high manufacturing yield even when errors occur that are larger than originally assumed.

In this initial demonstration, we performed the optimization on a fixed number of layers. However, the robust optimization problem can be viewed as providing a new cost function which takes into account robustness and, thus, can be used within other refinement algorithms, such as needle optimization [20], that allow for changing layer counts.

J. Birge received support from the Office of Naval Research under grant ONR N00014-02-1-0717 and the National Science Foundation under grant ECS-0501478.

References

1. R. Szipöcs, K. Ferencz, C. Spielmann, and F. Krausz, "Chirped multilayer coatings for broadband dispersion control in femtosecond lasers," *Opt. Lett.* **19**, 201–203 (1994).
2. F. X. Kärtner, N. Matuschek, T. Schibli, U. Keller, H. A. Haus, C. Heine, R. Morf, V. Scheuer, M. Tilsch, and T. Tschudi, "Design and fabrication of double-chirped mirrors," *Opt. Lett.* **22**, 831–833 (1997).
3. N. Matuschek, F. X. Kärtner, and U. Keller, "Theory of double-chirped mirrors," *IEEE J. Sel. Top. Quantum Electron.* **4**, 197–208 (1998).
4. F. X. Kaertner, U. Morgner, T. R. Schibli, E. P. Ippen, J. G. Fujimoto, V. Scheuer, G. Angelow, and T. Tschudi, "Ultra-broadband double-chirped mirror pairs for generation of octave spectra," *J. Opt. Soc. Am. B* **18**, 882–885 (2001).
5. B. Sullivan and J. Dobrowolski, "Deposition error compensation for optical multilayer coating: I. Theoretical description," *Appl. Opt.* **31**, 3821–3835 (1992).
6. V. Pervak, A. Tikhonravov, M. Trubetskov, S. Naumov, F. Krausz, and A. Apolonski, "1.5-octave chirped mirror for pulse compression down to sub-3 fs," *Appl. Opt.* **87**, 5–12 (2007).
7. V. Yakovlev and G. Tempea, "Optimization of chirped mirrors," *Appl. Opt.* **41**, 6514–6520 (2002).
8. A. Ben-Tal and A. Nemirovski, "Robust convex optimization," *Math. Oper. Res.* **23**, 769–806 (1998).
9. A. Ben-Tal and A. Nemirovski, "Robust optimization—methodology and applications," *Math. Program.* **92**, 453–480 (2002).
10. D. Bertsimas and M. Sim, "Robust discrete optimization and network flows," *Math. Program.* **98**, 49–71 (2003).
11. D. Bertsimas and M. Sim, "Tractable approximations to robust conic optimization problems," *Math. Program.* **107**, 5–36 (2006).
12. D. Bertsimas, O. Nohadani, and K. M. Teo, "Robust optimization in electromagnetic scattering problems," *J. Appl. Phys.* **101**, 074507 (2007).
13. J. A. Kong, *Electromagnetic Wave Theory* (EMW, 2000).
14. J. R. Birge and F. X. Kärtner, "Efficient analytic computation of dispersion from multilayer structures," *Appl. Opt.* **45**, 1478–1483 (2006).
15. J. R. Birge and F. X. Kärtner, "Efficient optimization of multilayer coatings for ultrafast optics using analytic gradients of dispersion," *Appl. Opt.* **46**, 2656–2662 (2007).
16. O. D. Mücke, R. Ell, A. Winter, J. Kim, J. R. Birge, L. Matos, and F. X. Kärtner, "Self-referenced 200 mHz octave-spanning ti:sapphire laser with 50 attosecond carrier-envelope phase jitter," *Opt. Express* **13**, 5163–5169 (2005).
17. D. Bertsimas, O. Nohadani, and K. M. Teo, "Robust optimization for unconstrained simulation-based problems," *Oper. Res.* (to be published).
18. P. Verly, "Fourier transform technique with refinement in the frequency domain for the synthesis of optical thin films," *Appl. Opt.* **35**, 5148–5154 (1996).
19. ILOG CPLEX, "High-performance software for mathematical programming and optimization," <http://www.ilog.com/products/cplex> (2007).
20. A. Tikhonravov, M. Trubetskov, and G. DeBell, "Applications of the needle optimization technique to the design of optical coatings," *Appl. Opt.* **35**, 5493–5508 (1996).